



Universiteit  
Leiden  
The Netherlands

## **T(1) relaxation in in vivo mouse brain at ultra-high field**

Ven, R.C.G. van de; Hogers, B.; Maagdenberg, A.M.J.M. van den; Groot, H.J.M. de; Ferrari, M.D.; Frants, R.R.; ... ; Kihne, S.R.

### **Citation**

Ven, R. C. G. van de, Hogers, B., Maagdenberg, A. M. J. M. van den, Groot, H. J. M. de, Ferrari, M. D., Frants, R. R., ... Kihne, S. R. (2007). T(1) relaxation in in vivo mouse brain at ultra-high field. *Magnetic Resonance In Medicine*, 58(2), 390-395.  
doi:10.1002/mrm.21313

Version: Publisher's Version

License: [Licensed under Article 25fa Copyright Act/Law \(Amendment Taverne\)](#)

Downloaded from: <https://hdl.handle.net/1887/3455130>

**Note:** To cite this publication please use the final published version (if applicable).

# $T_1$ Relaxation in In Vivo Mouse Brain at Ultra-High Field

Rob C.G. van de Ven,<sup>1</sup> Bianca Hogers,<sup>2</sup> Arn M.J.M. van den Maagdenberg,<sup>1,3</sup> Huub J.M. de Groot,<sup>4</sup> Michel D. Ferrari,<sup>3</sup> Rune R. Frants,<sup>1</sup> Robert E. Poelmann,<sup>2</sup> Louise van der Weerd,<sup>2\*</sup> and Suzanne R. Kiihne<sup>4</sup>

**Accurate knowledge of relaxation times is imperative for adjustment of MRI parameters to obtain optimal signal-to-noise ratio (SNR) and contrast. As small animal MRI studies are extended to increasingly higher magnetic fields, these parameters must be assessed anew. The goal of this study was to obtain accurate spin-lattice ( $T_1$ ) relaxation times for the normal mouse brain at field strengths of 9.4 and 17.6 T.  $T_1$  relaxation times were determined for cortex, corpus callosum, caudate putamen, hippocampus, periaqueductal gray, lateral ventricle, and cerebellum and varied from  $1651 \pm 28$  to  $2449 \pm 150$  ms at 9.4 T and  $1824 \pm 101$  to  $2772 \pm 235$  ms at 17.6 T. A field strength-dependent increase of  $T_1$  relaxation times is shown. The SNR increase at 17.6 T is in good agreement with the expected SNR increase for a sample-dominated noise regime. Magn Reson Med 58:390–395, 2007. © 2007 Wiley-Liss, Inc.**

**Key words:** magnetic field strength; longitudinal relaxation; spin-lattice relaxation; mouse; brain

Increasing knowledge of the mouse nervous system and the availability of a large number of transgenic models have made the mouse a very popular species in the study of neurological disorders. Noninvasive imaging techniques, such as MRI, have shown great potential to study brain pathology in these models (1,2). However, the small size of the mouse brain has considerable implications for obtaining a spatial resolution comparable to that routinely obtained with MRI in patients; the small voxel size used in mouse brain imaging results in a very low signal-to-noise ratio (SNR) at normal, medical field strengths ( $\leq 3$  T). Therefore, increasingly high magnetic field strengths (up to 17.6 T) are used to increase the SNR (3). Higher field strengths may also have positive effects on the contrast-to-

noise ratio, e.g., for the BOLD effect used in functional MRI, MRS, and magnetization transfer experiments (4,5).

The application of a higher field requires adjustment of image acquisition parameters, which are based on knowledge of the NMR tissue properties. Here, we focus on the spin-lattice relaxation time  $T_1$ , which can be used to assess neuropathology, such as tumors, multiple sclerosis, cerebral edema, and infarction (6).  $T_1$ -weighted imaging is also used extensively for contrast-enhanced MRI and to assess blood-brain-barrier integrity and perform molecular imaging (7). The field dependence of  $T_1$  may give considerable insight into the molecular origins of this image contrast mechanism, which will be useful in understanding how  $T_1$  is related to disease processes.

Reports on  $T_1$  relaxation times for mouse brain are limited mainly to systems of up to 11.7 T (8–10). Relaxation data of mouse brain at 17.6 T are lacking. In this study we aim at validating quantitative  $T_1$  imaging at high fields using phantoms. In addition, we provide in vivo  $T_1$  relaxation maps of mouse brain at 17.6 T and compare those with measurements at 9.4 T. The results are discussed in terms of field dependence of the in vivo  $T_1$  relaxation times and SNR.

## MATERIALS AND METHODS

### Phantoms

Phantom tubes were prepared by diluting a stock solution of 0.5 M Gadolinium-tetraazacycloDodecaneTetraacetic acid (Gd-DOTA) (Dotarem; Guerbet Nederland BV, Gorinchem, the Netherlands) in phosphate buffered saline. To produce a range of  $T_1$  values the following dilutions were used: 1:5000; 1:10,000; 1:25,000; 1:100,000; and 1:200,000. The  $T_1$  relaxation times were determined by both MRI and high-resolution NMR at field strengths of 9.4 and 17.6 T.

### Mice

In vivo imaging was performed on six female C57BL/6Jico mice aged 3 months (Charles River, Maastricht, the Netherlands). Before imaging, mice were initially anesthetized with 4% isoflurane in air (0.3 liters  $\text{min}^{-1}$ ) and  $\text{O}_2$  (0.3 liters  $\text{min}^{-1}$ ) and maintained with  $\sim 1.5\%$  isoflurane during all procedures. The respiratory rate was monitored via an air-pressure cushion connected to a laptop using Biotrig software (Bruker, Rheinstetten, Germany). The depth of the anesthesia was continuously regulated to maintain a stable respiration rate during each experiment. Body temperature of the animals was kept constant by pumping

<sup>1</sup>Department of Human Genetics, Leiden University Medical Center, Leiden, The Netherlands.

<sup>2</sup>Leiden MRM Facilities, Department of Anatomy, Leiden University Medical Center, Leiden, The Netherlands.

<sup>3</sup>Department of Neurology, Leiden University Medical Center, Leiden, The Netherlands.

<sup>4</sup>Leiden MRM Facilities, Leiden Institute of Chemistry, Leiden University, Leiden, The Netherlands.

Grant sponsor: Netherlands Organization for Scientific Research (NWO); Grant number: Vici 918.56.602; Grant sponsor: EU EUROHEAD; Grant number: LSHM-CT-2004-504837; Grant sponsor: Centre for Medical Systems Biology (CMSB), Netherlands Genomics Initiative/Netherlands Organization for Scientific Research (NGI/NWO).

Rob C.G. van de Ven and Bianca Hogers contributed equally to this work.

\*Correspondence to: Dr. Louise van der Weerd, Leiden MRM Facilities, Leiden Institute of Chemistry, Leiden University, PO Box 9502, 2300 RA Leiden, The Netherlands. E-mail: L.van\_der\_Weerd@lumc.nl

Received 14 June 2006; revised 23 April 2007; accepted 30 April 2007.

DOI 10.1002/mrm.21313

Published online in Wiley InterScience (www.interscience.wiley.com).

© 2007 Wiley-Liss, Inc.

warm water through the gradient system, resulting in a constant temperature of the animal bed of 26°C. Rectal temperature during the experiment was  $28.3 \pm 0.3^\circ\text{C}$ . All animal experiments were performed in accordance with the guidelines of the Leiden University and national legislation.

## MRI

Imaging was performed on two vertical 89-mm-bore magnets (Bruker BioSpin, Rheinstetten, Germany) with field strengths of 9.4 T (400 MHz) and 17.6 T (750 MHz). A Bruker Mini-0.5 gradient system of 200 mT/m and a transmit/receive birdcage radiofrequency coil with an inner diameter of 38 mm was used on both systems. Bruker ParaVision 3.0 software was used for image acquisition.

A multiple spin-echo saturation recovery method was used with variable repetition time (TR). Slice excitation and refocusing were accomplished by three-lobed sinc pulses with matched bandwidths, resulting in 90° and 180° pulse lengths of 1.0 and 0.81 ms, respectively. Imaging parameters were as follows: echo time (TE) = 3.5 ms; echoes = 8; TR-array at 9.4 T = 0.1, 0.12, 0.15, 0.3, 0.5, 0.9, 1.5, 3, 6, 12, and 20 s; TR-array at 17.6 T = 0.1, 0.12, 0.15, 0.3, 0.5, 0.9, 1.5, 3, 6, 10, and 30 s; matrix size =  $128 \times 128$ ; FOV = 25.6 mm; slice thickness = 1 mm. All images were acquired as single slices to avoid interslice modulation effects and unwanted stimulated echoes were suppressed by spoiler gradients in the slice direction. The slice was positioned through the center of all phantom tubes or dorsally through the middle of the cerebellum and rostrally through the olfactory bulb.

Although eight echoes were acquired to determine  $T_2$  relaxation times, the  $T_2$  values for the phantoms obtained at 17.6 T were extremely sensitive to processing parameters, did not show the expected  $T_2$  dependence upon Gd-DOTA concentration, and were shorter than the high-resolution NMR values by 50% or more. For these reasons, quantitative localized  $T_2$  measurements were not pursued in vivo.

## High-Resolution NMR

To validate the relaxation time measurements, relaxation rates in the phantoms were obtained by both MRI and high-resolution NMR. The same phantoms and magnets were used and experiments were performed on the same day. Radiation damping was avoided in the high-resolution experiments by using a restricted sample volume in untuned, probes with a low quality-factor at both field strengths. A broadband 5-mm solution-state NMR probe with a 120-μl sample tube was used at 9.4 T, while a triple-tuned magic-angle spinning probe with a 400-μl sample holder was used at 17.6 T.

$T_1$  was measured using an inversion recovery spin-echo experiment. The 90° and 180° pulse lengths were 25 and 50 μs, respectively. We used a variable list of 11 inversion times that were changed appropriately to the expected  $T_1$  of each sample. Both TR and the longest inversion time were kept at  $>10 \times$  the expected  $T_1$  of the sample.

## Relaxation Analysis by MRI

Phase correction was performed on the entire complex data matrix using the linear zero- and first-order phase

procedure in Bruker Paravision 3.0. Regions of interest (ROIs) were defined bilaterally for each individual mouse in cortex, corpus callosum, caudate putamen, hippocampus, periaqueductal gray, lateral ventricle, and cerebellum. The relaxation curves were phased to avoid baseline artifacts (11) and the real part was used for the relaxation fits. For the  $T_1$  fits, 11 TR values with a fixed TE of 7 ms (second echo) were used. The  $T_1$  values of the various ROIs were determined using a three-parameter SR fit function:

$$M(t) = A + M_0(1 - \exp(-t/T_1)), \quad [1]$$

where  $M_0$  is the equilibrium magnetization. All fits were performed using a nonlinear least square algorithm provided by the Image Sequence Analysis (ISA) tool of ParaVision 3.02.  $T_1$  maps were generated on a pixel-by-pixel basis with the ISA tool.

## Relaxation Analysis by High-Resolution NMR

Spectra were line-broadened (10 Hz Lorentzian) and Fourier-transformed. The zeroth order phase was adjusted on the time point with the highest SNR and the same phase parameters were applied to all spectra in the experiment. Maximal intensities were detected automatically and fitted to a three-parameter inversion recovery equation:

$$M(t) = M_0(1 - 2\alpha\exp(-t/T_1)), \quad [2]$$

where  $\alpha$  is the inversion angle.

## SNR

SNR was calculated by placing a ROI in the tissue of interest and comparing the mean signal intensity ( $SI$ ) with the SD of the noise obtained from a large ROI placed in the image background, outside the mouse,

$$\text{SNR} = \frac{SI}{\text{SD}_{\text{noise}}}.$$

## Statistics

$T_1$  times at 9.4 and 17.6 T were compared by two-way repeated measures analysis of variance (ANOVA).  $T_1$  times of the different ROIs were compared by averaging the results of the left and right hemisphere for each individual animal, after which an unpaired two-tailed Student's  $t$ -test with Bonferroni-Holmes correction for multiple comparisons was done. Statistical analyses were performed using SPSS software (version 11; Chicago, IL, USA). Data is presented as mean  $\pm$  SD.

## RESULTS

### Phantoms

Gd-DOTA phantoms of various concentrations were prepared to validate the MRI protocol for  $T_1$  measurements against a standard inversion recovery high-resolution NMR protocol. At 9.4 T no significant differences were found between the MRI results and the high-resolution NMR results (Fig. 1). At 17.6 T the imaging method yielded

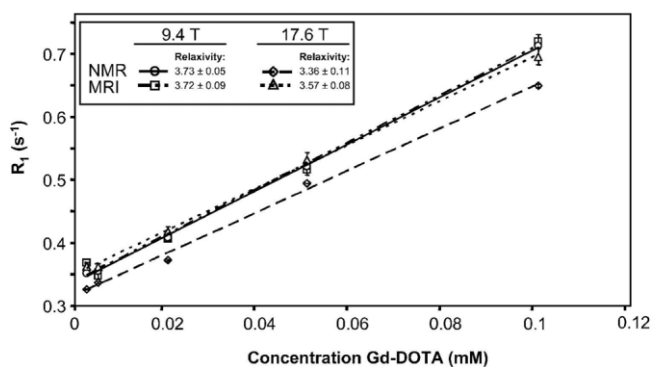


FIG. 1. Relaxation measurements of phantoms using imaging and high-resolution NMR.  $R_1$  relaxation rates as a function of Gd-DOTA concentration yields relaxivity. Mean  $R_1$  in  $s^{-1} \pm$  error bars (SD). Relaxivity in  $mM^{-1} s^{-1} \pm$  SD.

$T_1$  values that were consistently 10% shorter than for the high-resolution NMR method. Despite these differences, a plot of  $R_1$  vs. the Gd-DOTA concentration yields straight lines with similar slopes for the two methods (Fig. 1). The Gd-DOTA relaxivities determined from the slopes are also given in Fig. 1. At 9.4 T, the Gd-DOTA relaxivity was about 10% higher than the manufacturer's value at 1.5 T of  $3.4 mM^{-1} s^{-1}$ ; at 17.6 T the relaxivity was decreased by about 9% compared to 9.4 T.

## Mice

$T_1$  relaxation times were determined in vivo at 9.4 and 17.6 T. ROIs were selected in cortex, corpus callosum, caudate putamen, hippocampus, periaqueductal gray, lateral ventricle, and cerebellum (Fig. 2a). Table 1 summarizes the  $T_1$  relaxation times calculated from these ROIs. Within this study,  $T_1$  times significantly increase with field strength (two-way repeated measures ANOVA,  $P = 0.018$ ). Additionally,  $T_1$  maps were generated on a pixel-by-pixel basis (Fig. 2b and c).

We also performed a literature study to compare  $T_1$  relaxation in rodent (8–10,12–24) and human (25–38)

brain for different field strengths (Fig. 3). Our data tie in well with previous data on rodent gray and white matter. Due to limited data points per field strength, the variation in protocols between the literature sources and the theoretical nonlinearity of field-dependent  $T_1$  increase, it is not informative to perform statistical analysis on the data presented in Fig. 3a and b. Nonetheless, there clearly is a positive trend toward increasing  $T_1$  times—for both gray and white matter in both rodents and humans—with field strength. Based on Fig. 3c and d, there is no statistical evidence that either the absolute or the relative difference in  $T_1$  between gray and white matter changes with increasing field strength. Interestingly, the gray and white matter difference in  $T_1$  is significantly larger in humans ( $P = 0.0001$ ).

## SNR

The SNR performance of both imaging field strengths was compared for the mouse data. For all mice, the SNR was calculated using a ROI in the cortex on the second echo in every SE data set (proton density-weighted image; TE = 7 ms and TR = 20 or 30 s). The average experimental increase in SNR between 9.4 T and 17.6 T was  $1.95 \pm 0.09$ . This increase may be slightly underestimated because of a decrease in  $T_2$  at higher field. Nonetheless, these values are in good agreement with expected SNR increase for a sample-dominated noise regime ( $SNR \propto B_0 = 17.6/9.4 = 1.87$ ).

## DISCUSSION AND CONCLUSIONS

### Relaxation Times

Here we report  $T_1$  relaxation times of mouse brain at both 9.4 and 17.6 T. These results are obtained on the same mice using consistent protocols, allowing direct comparison of measurements. The in vivo  $T_1$  relaxation times are obtained for specific mouse brain regions, allowing comparison with other studies at different field strengths. These data can be used for optimization of high-field imaging protocols. They also provide baseline values for

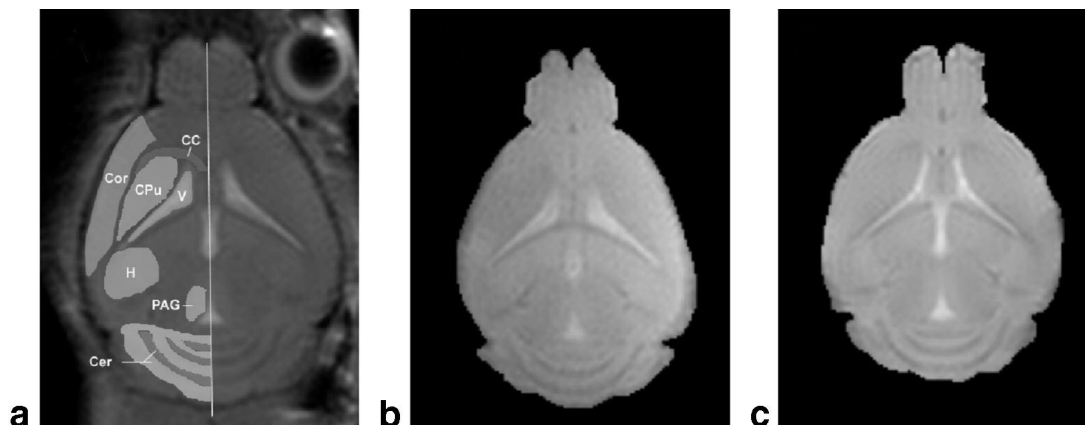


FIG. 2. ROIs selected in a single  $T_2$ -weighted spin-echo image (a). CC, corpus callosum; Cer, cerebellum; Cor, cortex; CPu, caudate putamen; H, hippocampus; PAG, periaqueductal gray; V, lateral ventricle.  $T_1$  maps at 9.4 T (b) and 17.6 T (c) are depicted. The images are calculated from monoexponential fits to 11 SR images with TE of 7 ms and TRs ranging from 100 ms to 20 s at 9.4 T or 30 s at 17.6 T.

Table 1  
In Vivo T<sub>1</sub> Relaxation Times of Mouse Brain at 9.4 and 17.6 T\*

	CC	Cor	H	PAG	CPu	V	CerG	CerW
9.4 T	1.75 ± 0.05	1.89 ± 0.12	1.82 ± 0.05	1.70 ± 0.07	1.75 ± 0.03	2.45 ± 0.20	1.81 ± 0.12	1.65 ± 0.03
17.6 T	1.83 ± 0.09	2.03 ± 0.11	1.90 ± 0.08	1.84 ± 0.11	1.82 ± 0.10	2.77 ± 0.24	2.04 ± 0.06	1.89 ± 0.11
Factor increase	1.05	1.07	1.04	1.08	1.04	1.13	1.12	1.14

\* Mean relaxation times in s ± SD. CC = corpus callosum, CerG = cerebellum gray matter, CerW = cerebellum white matter, Cor = cortex, Cpu = caudate putamen, H = hippocampus, PAG = periaqueductal gray, V = ventricle.

relaxation times obtained in pathology in (transgenic) mice.

Published NMR relaxation values in rodent and human brain are scarce. We summarized available data in Fig. 3. This figure clearly shows the large variation in the reported values, which is caused by different hardware, pulse sequences and protocols, mouse and rat strains, age, fitting procedures, etc. In our measurements, care was taken to avoid most of the mentioned constraints in order to obtain the fairest comparison possible between the different magnetic field strengths. In particular, we note that careful phasing and the use of real data are required to minimize baseline effects and obtain quantitative agreement with high-resolution NMR methods (11). Despite the variability in T<sub>1</sub> values, it is obvious that T<sub>1</sub> increases with increasing field strength for both rodent and human brain. In studies with matched protocols at different field strengths, a significant increase of T<sub>1</sub> was always found with field strength (e.g., this study, 31,38). Interestingly, the difference in gray matter T<sub>1</sub> and white matter T<sub>1</sub> is larger in humans than in rodents at every field strength. This may be due to differences in cytoarchitecture between the species, with humans, e.g., having a lower neuron density (39). Also, the rodent measurement were all performed under anesthetics, which are known to change

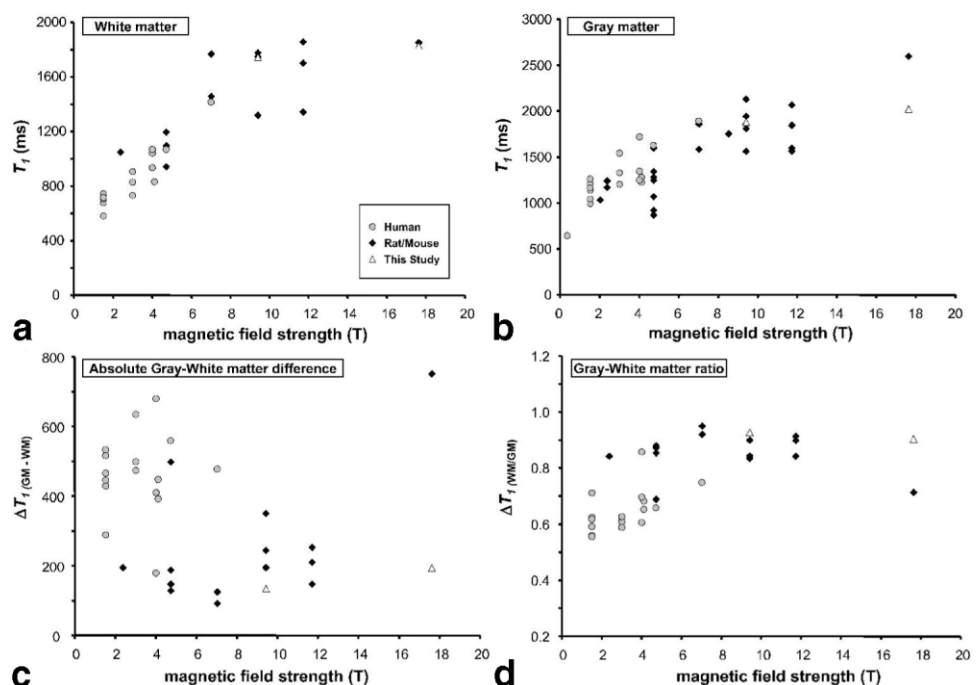
tissue perfusion (40) and can thereby affect the T<sub>1</sub> measurements, particularly in the gray matter.

The measured T<sub>1</sub> values will be slightly underestimated because of the low body temperature during the experiments. However, since all experiments were performed under the same temperature regime, we feel that all conclusions regarding T<sub>1</sub> increase and dispersion with field strength are valid.

We and others have observed signal irreproducibility in ultra-high field T<sub>2</sub> measurements (41). Several groups are currently looking into this spin turbulence phenomenon, which appears to involve radiation damping and/or intermolecular multiple quantum effects, both of which will be large in these essentially aqueous samples at high field (42,43). This is beyond the scope of this paper, and we refer to the work of Datta et al. (42) and Huang et al. (43) for a theoretical discussion of these processes.

Experimentally, a spin-echo experiment is intrinsically more susceptible to spin turbulence than an IR or SR experiment, due to the longer time spent by the spins in the transverse plane. Especially small pulse imperfections may have a huge effect on signal evolution in an SE experiment (42). For the T<sub>1</sub> measurement, we chose an SR sequence, which yields less signal in the transverse plane in order to minimize radiation damping effects. For the

FIG. 3. Magnetic field dependence of T<sub>1</sub>. White (a) and gray (b) matter T<sub>1</sub> values in rodent (mouse and rat, black diamonds) and human (gray squares) brain are plotted based on literature data (8–10,12–37) and the experimental data from this study (white triangles). Absolute gray-white matter differences were calculated by subtraction of gray and white matter T<sub>1</sub> values of the same study (c). Relative gray-white matter ratios were calculated by dividing white and gray matter T<sub>1</sub> values of the same study (d).





high-resolution  $T_1$  measurements we purposely used an untuned probe with a low quality-factor, but it is still possible that radiation damping is the cause of the small discrepancy in  $T_1$  at 17.6 T. Even so, the  $T_1$  measurements still yield consistent and reproducible values.

## SNR

The use of high magnetic field results in increased SNR. Some advantages are that shorter acquisition times may be used and spatial resolution increased. The observed SNR increase at higher field depends on field strength and on the sample size and properties relative to the coil size. For very small samples, coil noise predominates, resulting in a field dependence of  $\text{SNR} \propto B_0^{7/4}$  (44). For large conductive samples, such as living mice, the sample noise dominates over coil noise, in particular at high magnetic fields and large sample diameter. Under these limiting conditions, the noise increases linearly with resonance frequency and thus  $\text{SNR} \propto B_0$  (45). The SNR increase in images of mouse brain was 1.95, which is in good agreement with expected SNR increase for a sample-dominated noise regime ( $\text{SNR} \propto B_0 = 17.6/9.4 = 1.87$ ).

## Field Dependence

An understanding of relaxation processes at the molecular level can provide a link between image intensity and tissue viability or biological processes. It is well known that the observed water  $T_1$  relaxation in tissues is dominated by the much shorter  $T_1$  relaxation of protons on macromolecules that are in contact with exchanging water molecules (46,47). Relaxation theory predicts that  $T_1$  increases with increasing field strength and eventually reaches a plateau at the solvent  $T_1$ . The  $T_1$  of water is practically flat over the full range of NMR accessible measurements (except for the small effects of dissolved paramagnetic oxygen). At 17.6 T, we measured a  $T_1$  of tap water of 3.3 s, which is significantly longer than the observed tissue  $T_1$ . The continuing  $T_1$  difference indicates that the local magnetic field of the in vivo water protons is modulated at high frequencies, enabling relatively efficient relaxation when compared to the solvent.

In conclusion, we have determined regional  $T_1$  values of mouse brain in vivo at 9.4 and 17.6 T. The results show that  $T_1$  still increases with field strength at ultra-high magnetic fields. The large gain in SNR encourages the use of ultra-high fields and merits further work in this direction.

## ACKNOWLEDGMENTS

We thank Fons Lefeber and Kees Erkelens for technical assistance. This work was supported by a grant from the Netherlands Organization for Scientific Research (NWO) (Vici 918.56.602; to M.D.F), the EU EUROHEAD grant (LSHM-CT-2004-504837; to M.D.F, R.R.F, A.M.J.M.v.d.M), and the Centre for Medical Systems Biology (CMSB) established by the Netherlands Genomics Initiative/Netherlands Organisation for Scientific Research (NGI/NNO)

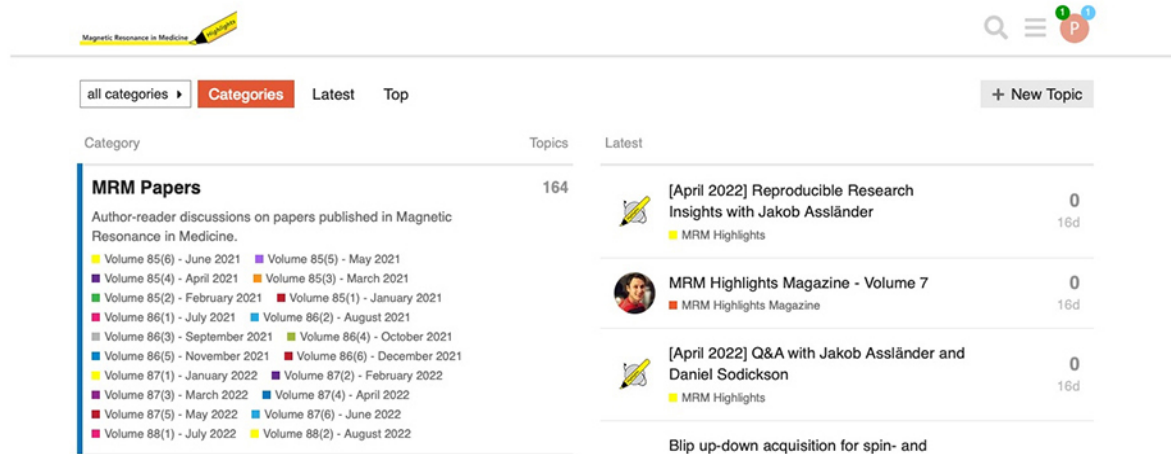
## REFERENCES

- Choi IY, Lee SP, Guilfoyle DN, Helpert JA. In vivo NMR studies of neurodegenerative diseases in transgenic and rodent models. *Neurochem Res* 2003;28:987–1001.
- Van der Weerd L, Thomas DL, Thornton JS, Lythgoe MF. MRI of animal models of brain disease. *Methods Enzymol* 2004;386:149–177.
- Hu X, Norris DG. Advances in high-field magnetic resonance imaging. *Annu Rev Biomed Eng* 2004;6:157–184.
- Benveniste H, Blackband S. MR microscopy and high resolution small animal MRI: applications in neuroscience research. *Prog Neurobiol* 2002;67:393–420.
- Hennig J, Speck O, Koch MA, Weiller C. Functional magnetic resonance imaging: a review of methodological aspects and clinical applications. *J Magn Reson Imaging* 2003;18:1–15.
- Tofts PS.  $T_1$ : the longitudinal relaxation time. In: Tofts PS, editor. *Quantitative MRI of the brain*. Chichester: John Wiley and Sons; 2003. p 111–142.
- Dijkhuizen RM, Nicolay K. Magnetic resonance imaging in experimental models of brain disorders. *J Cereb Blood Flow Metab* 2003;23:1383–1402.
- Guilfoyle DN, Dyakin VV, O'Shea J, Pell GS, Helpert JA. Quantitative measurements of proton spin-lattice ( $T_1$ ) and spin-spin ( $T_2$ ) relaxation times in the mouse brain at 7.0 T. *Magn Reson Med* 2003;49:576–580.
- Kuo YT, Herlihy AH, So PW, Bhakoo KK, Bell JD. In vivo measurements of  $T_1$  relaxation times in mouse brain associated with different modes of systemic administration of manganese chloride. *J Magn Reson Imaging* 2005;21:334–339.
- Lee JH, Silva AC, Merkle H, Koretsky AP. Manganese-enhanced magnetic resonance imaging of mouse brain after systemic administration of  $\text{MnCl}_2$ : dose-dependent and temporal evolution of  $T_1$  contrast. *Magn Reson Med* 2005;53:640–648.
- van der Weerd L, Vergeldt FJ, Adrie de Jager P, Van As H. Evaluation of algorithms for analysis of NMR relaxation decay curves. *Magn Reson Imaging* 2000;18:1151–1158.
- Calamante F, Lythgoe MF, Pell GS, Thomas DL, King MD, Busza AL, Sotak CH, Williams SR, Ordidge RJ, Gadian DG. Early changes in water diffusion, perfusion,  $T_1$ , and  $T_2$  during focal cerebral ischemia in the rat studied at 8.5 T. *Magn Reson Med* 1999;41:479–485.
- De Graaf RA, Brown PB, McIntyre S, Nixon TW, Behar KL, Rothman DL. High magnetic field water and metabolite proton  $T_1$  and  $T_2$  relaxation in rat brain in vivo. *Magn Reson Med* 2006;56:386–394.
- Eis M, Els T, Hoehn-Berlage M. High resolution quantitative relaxation and diffusion MRI of three different experimental brain tumors in rat. *Magn Reson Med* 1995;34:835–844.
- Hoehn-Berlage M, Eis M, Back T, Kohno K, Yamashita K. Changes of relaxation times ( $T_1$ ,  $T_2$ ) and apparent diffusion coefficient after permanent middle cerebral artery occlusion in the rat: temporal evolution, regional extent, and comparison with histology. *Magn Reson Med* 1995;34:824–834.
- Massicotte EM, Buist R, Del Bigio MR. Altered diffusion and perfusion in hydrocephalic rat brain: a magnetic resonance imaging analysis. *J Neurosurg* 2000;92:442–447.
- Padgett KR, Blackband SJ, Grant SC. Native  $T_1$  contrast enhancement at 4.7, 11 and 17.6 T for neuroimaging. In: *Proceedings of the 13th Annual Meeting of ISMRM*, Miami Beach, FL, USA, 2005 (Abstract 2198).
- Rajan SS, Rosa L, Francisco J, Muraki A, Carvlin M, Tuturea E. MRI characterization of 9L-glioma in rat brain at 4.7 Tesla. *Magn Reson Imaging* 1990;8:185–190.
- Schwarcz A, Berente Z, Osz E, Doczi T. In vivo water quantification in mouse brain at 9.4 Tesla in a vasogenic edema model. *Magn Reson Med* 2001;46:1246–1249.
- Schwarcz A, Berente Z, Osz E, Doczi T. Fast in vivo water quantification in rat brain oedema based on  $T(1)$  measurement at high magnetic field. *Acta Neurochir (Wien)* 2002;144:811–815.
- Ting YL, Bendel P. Thin-section MR imaging of rat brain at 4.7 T. *J Magn Reson Imaging* 1992;2:393–399.
- Van der Weerd L, Lythgoe MF, Badin RA, Valentim LM, Akbar MT, De Bellerche JS, Latchman DS, Gadian DG. Neuroprotective effects of HSP70 overexpression after cerebral ischaemia—an MRI study. *Exp Neurol* 2005;195:257–266.
- Van Dorsten FA, Olah L, Schwindt W, Grune M, Uhlenkuken U, Pillekamp F, Hossmann KA, Hoehn M. Dynamic changes of ADC, perfusion, and NMR relaxation parameters in transient focal ischemia of rat brain. *Magn Reson Med* 2002;47:97–104.
- Zaharchuk G, Hara H, Huang PL, Fishman MC, Moskowitz MA, Jenkins BG, Rosen BR. Neuronal nitric oxide synthase mutant mice show smaller infarcts and attenuated apparent diffusion coefficient changes in the peri-infarct zone during focal cerebral ischemia. *Magn Reson Med* 1997;37:170–175.

25. Barfuss H, Fischer H, Hentschel D, Ladebeck R, Vetter J. Whole-body MR imaging and spectroscopy with a 4-T system. *Radiology* 1988;169:811–816.
26. Breger RK, Rimm AA, Fischer ME, Papke RA, Haughton VM. T<sub>1</sub> and T<sub>2</sub> measurements on a 1.5-T commercial MR imager. *Radiology* 1989;171:273–276.
27. Fan G, Wu Z, Pan S, Guo Q. Quantitative study of MR T<sub>1</sub> and T<sub>2</sub> relaxation times and 1H MRS in gray matter of normal adult brain. *Chin Med J (Engl)*. 2003;116:400–404.
28. Jezzard P, Duewell S, Balaban RS. MR relaxation times in human brain: measurement at 4 T. *Radiology* 1996;199:773–779.
29. Kim SG, Hu X, Ugurbil K. Accurate T<sub>1</sub> determination from inversion recovery images: application to human brain at 4 Tesla. *Magn Reson Med* 1994;31:445–449.
30. Kwag JH, Zhang X, Zhu XH, Andersen P, Ugurbil K, Chen W. Fast mapping of T<sub>1</sub> relaxation times in the human brain gray and white matters at 7 Tesla. In: *Proceedings of the 9th Annual Meeting of ISMRM, Glasgow, Scotland, 2001 (Abstract 1346)*.
31. Lu H, Nagae-Poetscher LM, Golay X, Lin D, Pomper M, van Zijl PC. Routine clinical brain MRI sequences for use at 3.0 Tesla. *J Magn Reson Imaging* 2005;22:13–22.
32. Mason GF, Chu WJ, Hetherington HP. A general approach to error estimation and optimized experiment design, applied to multislice imaging of T<sub>1</sub> in human brain at 4.1 T. *J Magn Reson* 1997;126:18–29.
33. Schmitt P, Griswold MA, Jakob PM, Kotas M, Gulani V, Haase A. Inversion recovery TrueFISP: quantification of T(1), T(2), and spin density. *Magn Reson Med* 2004;51:661–667.
34. Takaya N, Watanabe H, Mitsumori F. Elongated T<sub>1</sub> values in human brain and the optimization of MDEFT measurements at 4.7T. In: *Proceedings of the 12th Annual Meeting of ISMRM, Kyoto, Japan, 2004 (Abstract 2339)*.
35. Van Walderveen MA, Van Schijndel RA, Pouwels PJ, Polman CH, Barkhof F. Multislice T<sub>1</sub> relaxation time measurements in the brain using IR-EPI: reproducibility, normal values, and histogram analysis in patients with multiple sclerosis. *J Magn Reson Imaging* 2003;18:656–664.
36. Vrenken H, Geurts JJ, Knol DL, Van Dijk LN, Dattola V, Jasperse B, Van Schijndel RA, Polman CH, Castelijns JA, Barkhof F, Pouwels PJ. Whole-brain T<sub>1</sub> mapping in multiple sclerosis: global changes of normal-appearing gray and white matter. *Radiology* 2006;240:811–820.
37. Wansapura JP, Holland SK, Dunn RS, Ball Jr WS. NMR relaxation times in the human brain at 3.0 Tesla. *J Magn Reson Imaging* 1999;9:531–538.
38. Weigel M, Hennig J. Contrast behavior and relaxation effects of conventional and hyperecho-turbo spin echo sequences at 1.5 and 3 T. *Magn Reson Med* 2006;55:826–835.
39. DeFelipe J, Alonso-Nanclares L, Arellano JI. Microstructure of the neocortex: comparative aspects. *J Neurocytol* 2002;31:299–316.
40. Stullken Jr EH, Milde JH, Michenfelder JD, Tinker JH. The nonlinear responses of cerebral metabolism to low concentrations of halothane, enflurane, isoflurane, and thiopental. *Anesthesiology* 1977;46:28–34.
41. Huang SY, Walls JD, Wang Y, Warren WS, Lin YY. Signal irreproducibility in high-field solution magnetic resonance experiments caused by spin turbulence. *J Chem Phys* 2004;121:6105–6109.
42. Datta S, Huang SY, Lin YY. The transient dynamics leading to spin turbulence in high-field solution magnetic resonance: a numerical study. *J Chem Phys* 2006;124:154501.
43. Huang SY, Wolahan SM, Mathern GW, Chute DJ, Akhtari M, Nguyen ST, Huynh MN, Salamon N, Lin YY. Improving MRI differentiation of gray and white matter in epileptogenic lesions based on nonlinear feedback. *Magn Reson Med* 2006;56:776–786.
44. Mansfield P, Morris PG. Waugh JS, editors. *NMR imaging in biomedicine*. New York: Academic Press; 1982.
45. Edelstein WA, Glover GH, Hardy CJ, Redington RW. The intrinsic signal-to-noise ratio in NMR imaging. *Magn Reson Med* 1986;3:604–618.
46. Bryant RG. The dynamics of water-protein interactions. *Annu Rev Biophys Biomol Struct* 1996;25:29–53.
47. Koenig SH, Brown 3rd RD, Adams D, Emerson D, Harrison CG. Magnetic field dependence of 1/T<sub>1</sub> of protons in tissue. *Invest Radiol* 1984;19:76–81.

# WOULD YOU LIKE TO POST AN INFORMAL COMMENT ABOUT THIS PAPER, OR ASK THE AUTHORS A QUESTION ABOUT IT?

If so, please visit <https://mrm.ismrm.org/> and register for our Magn Reson Med Discourse site (registration is free).



The screenshot shows the Magn Reson Med Discourse website. At the top, there is a search bar and a navigation menu with 'all categories', 'Categories', 'Latest', and 'Top'. Below the navigation, there is a 'New Topic' button. The main content area is divided into two columns. The left column, titled 'Category', lists various issues of the journal, including 'MRM Papers' and 'MRM Highlights Magazine'. The right column, titled 'Topics', shows a list of topics with their respective counts and dates. The topics listed are '[April 2022] Reproducible Research Insights with Jakob Assländer', 'MRM Highlights Magazine - Volume 7', and '[April 2022] Q&A with Jakob Assländer and Daniel Sodickson'. Each topic has a count of 0 and a date of 16d.

Magn Reson Med is currently listing the top 8 downloaded papers from each issue (including Editor's Picks) for comments and questions on the Discourse web site.

However, we are happy to list this or any other papers (please email [mrm@ismrm.org](mailto:mrm@ismrm.org) to request the posting of any other papers.)

We encourage informal comment and discussion about Magn Reson Med papers on this site. Please note, however, that a formal errata from the authors should still be submitted in the usual way via our Manuscript Central online submission system.